Journal of Innovative Technology, Vol. 4, No. 2, pp. 13-19, September 2022
http://doi.org/10.29424/JIT.202209_4(2).0002

FEM Design and Implementation of a Novel Linear Motor for Fluid-Power Proportional Valves

Chin-Yi Cheng [1*], Jyh-Chyang Renn [2], Ilham Saputra [3], Chen-En Shi [3]

ABSTRACT

In this paper, a novel short-stroke linear motor for fluid power proportional valve technology is proposed and realized. One most innovative design of the proposed linear motor is the movable pair of permanent magnets that are directly embedded into the output plunger of armature. Compared to the commonly used linear motor, in which the pair of permanent magnets are generally integrated into the stator and hence are not movable, this novel design realizes the linear output force/stroke characteristic. During the design process, the electro-magnetic software FLUX 2D is utilized as a tool to develop the novel linear motor. In addition, a prototype is also successfully manufactured. Finally, experimental results show that the effective linear working stroke of the novel linear motor is around ± 1.0 mm and the maximal output force reaches ± 16 N for the rated excitation current of ± 1.0A. Such a novel linear motor has the potential to replace the traditional proportional solenoid and is expected to find some real applications in future fluid power proportional valve technology.

Keywords: Linear-motor, Fluid Power, Proportional valve, Electro-magnetic.

1. INTRODUCTION

Nowadays, electro-mechanical transducers are widely used in the design of electro-hydraulic and electro-pneumatic valves (Backe, 1993; Renn & Xu, 2003). Thus, various of electro-hydraulic and electro-pneumatic valves have been proposed so far (Melin & Quake, 2007; Sugioka, 2010; Mohith, Karanth & Kulkarni, 2019). Among these different electro-mechanical transducers, the switching solenoid is perhaps the most commonly used one and has been widely applied to the design of conventional fluid power on-off solenoid valves. On the other hand, the proportional solenoid has been successfully applied to the design of fluid power proportional valves. Fig. 1 shows the schematic comparison between the switching and proportional solenoid (Renn & Xu, 2003). Obviously, the static force/stroke relation of the latter is linear, though these two different solenoids possess almost the same structure (Renn & Xu, 2003; Renn & Tsai, 2002; Gamble & Tappe, 2008). In details, the linear force/stroke relation of the proportional solenoid is the key requirement for the design of a fluid power proportional valve (Backe, 1993). The spool, which is subjected to a constant force within the linear working stroke, reaches a definite position in the valve body according to Hook's law. This definite position of the spool signifies a definite opening area of the valve orifice. Therefore, the volumetric flow-rate may be varied continuously by electrically adjusting the opening area of the proportional valve orifice.

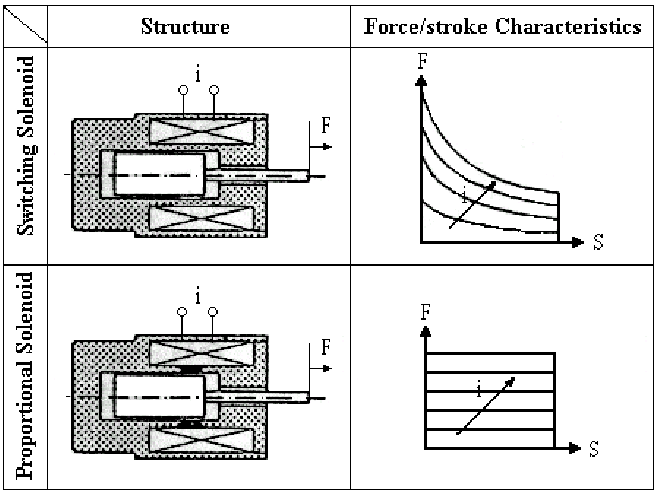

Fig. 1 Schematic comparison between the switching and proportional solenoid [1, 2].

As for the short-stroke linear motor, after surveying some previous reports, a most commonly used structure is found and depicted in Fig. 2. In which the pair of permanent magnets are integrated into the stator and hence are not movable. In addition, its nonlinear force/stroke characteristic limits such a linear motor to be applied to the design of fluid power on-off valve only (Backe, 1993; Renn & Xu, 2003). Another relevant but different linear force motor is found with application to electro-hydraulic valves. A remarkable feature of the linear force motor is its bi-directional force output. However, its force/stroke characteristic is still nonlinear. Besides, its complex construction increases inevitably the cost and difficulty in maintenance (Li, Ding & Wang, 2005). An

Manuscript received March 29, 2022; revised June 24, 2022; accepted July 5, 2022.
[1*] Assistant Professor (corresponding author), Department of Mechanical Engineering, National Yunlin University of Science and Technology, Taiwan (zezheng@yuntech.edu.com)
[2] Professor, Department of Mechanical Engineering, National Yunlin University of Science and Technology, Taiwan.
[3] Ph.D. Student, Department of Mechanical Engineering, National Yunlin University of Science and Technology, Taiwan.

interesting application of a short-stroke linear motor to a miniature pump is found in the literature as well. The linear motor serves as the main mechanism to drive the piston of the pump to move back and forth. Its force/stroke characteristic is actually not the major design consideration and is naturally nonlinear (Yamahata et al., 2005). So far, the short-stroke linear motor is basically not an option for the design of fluid power proportional valve because of its inherent nonlinear output force/stroke relation. In addition, as mentioned by Zimmermann and colleagues (2021), the calculation for friction also allows for describing the vibration-induced rod displacement process in a linear motor with higher accuracy. In this paper, therefore, a novel short-stroke linear motor for fluid power proportional valve is proposed and realized. Two significant features of the newly developed linear motor are the quite linear force/stroke characteristic and the movable pair of permanent magnets that are directly embedded into the output plunger of the armature. Let us start with the initial design concept of the novel linear motor as shown in Fig. 3. The coil is wound around the bakelite to generate the control magnetic flux. However, the permanent magnet on each side of the plunger produces its own magnetic flux as well. In Fig. 3, the chain line shows the magnetic flux of the permanent magnet and the dotted line indicates the magnetic flux due to magnetomotive force proportional to the input control current. Consequently, the control and the permanent magnetic fluxes are added on the left-hand side of the plunger while both are canceled on the right-hand side of the plunger. Therefore, the developed magnetic force drives the plunger to move to the right. Similarly, if a negative control current is given to the coil, then the plunger will be driven by the developed magnetic force to move to the left. Thus, the proposed linear motor is able to provide bi-directional force output. In addition, it is possible to achieve a linear force/stroke characteristic as long as the design dimensions are properly determined. The detailed schematic layout of the proposed novel linear motor is shown in Fig. 4. It is observed that two cylindrical permanent magnets are embedded into both ends of the movable plunger respectively. Such an innovative design, therefore, is totally different from the common linear motor as shown in Fig. 2. The chosen magnetic materials and permanent magnets are also depicted in Fig. 4. To achieve the linear force/stroke characteristic, the commercial FLUX 2D software is utilized as a tool to obtain the most suitable dimension for the linear motor. In the following, the design procedure using FLUX 2D is briefly outlined.

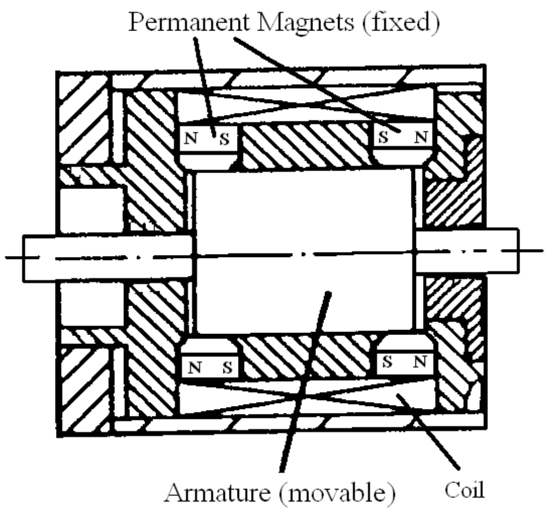

Fig. 2 Structure of the commonly used linear motor [1].

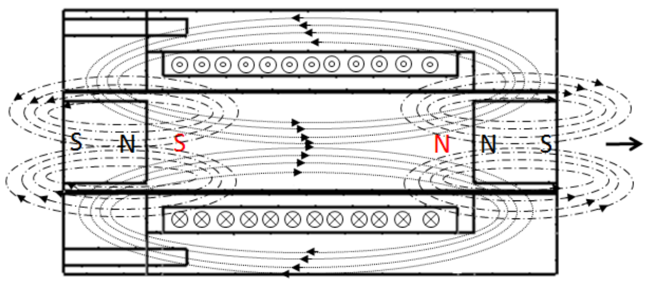

Fig. 3 The initial design concept of the novel linear motor.

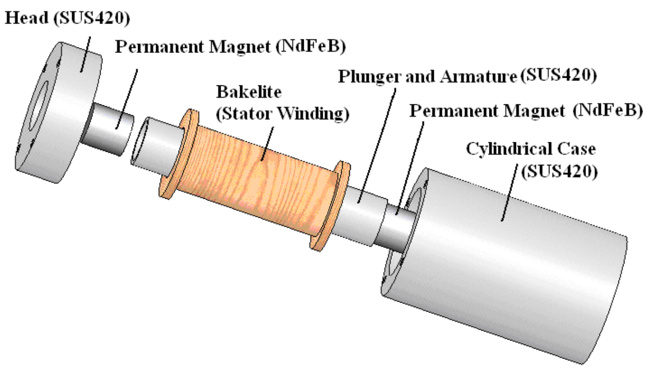

Fig. 4 Layout of the proposed novel linear motor.

2. DESIGNING THE LINEAR MOTOR USING FLUX 2D

In this paper, the commercial FEM software package FLUX 2D is chosen as a tool to design the electro-mechanical linear motor. Generally speaking, conventional design approach based on equivalent circuit method and trial-and-error are time-consuming (Renn & Xu, 2003). However, the introduction of FLUX 2D helps to test new ideas quickly and designs rapidly a successful prototype. In this paper, we mainly use the FEA Flux software to simulate and analyze the electromagnetic effect, and the analysis results are generated by geometry, mesh creation, material parameter setting, driving current and other setting items, then the force and displacement relationship curve can be generated to understand the variation of The results are analyzed by geometry, mesh creation, material parameter setting, drive current, etc. Fig 5. as show the Flowchart of Finite Element Analysis Flux software.

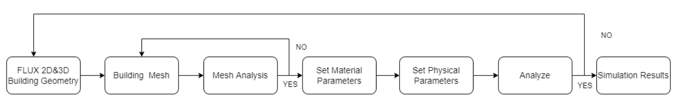

Fig. 5 Flowchart of Finite Element Analysis Flux software.

Fig. 6 as shows the construction of the study domain by creating the necessary points. Since the geometry of the linear motor is axis-symmetric, a two-dimensional cylindrical coordinate model of the magnetic field is established for the quantitative analysis of the plunger's output force. The FLUX 2D's automatic mesh generator then accomplishes the meshing in finite elements as shown in Fig. 6. In this Figure 6, the direction of movement is upward when the positive voltage is applied. Therefore, the mesh segmentation of the finite elements has a higher density in the lower mesh, mainly to observe the relationship between the flux density and the displacement when the positive voltage is applied. Before the simulations, the value of the excitation current as well as the magnetization (B-H) curves for different magnetic materials must be given in advance. The former is the known input signal and the latter can be found in the catalogs of corresponding magnetic materials. In addition, the boundary condition assuming all the field lines are perpendicular to the boundary is applied throughout the simulations. It is also worth mentioning that, in order to obtain the output magnetic force as large as possible, the permanent magnet made of a high magnetic rare-earth material (NdFeB) is chosen. The corresponding remnant flux density is around 1.45 Tesla. The diameter of the coil-wire is 0.3mm and the number of turns of the coil is 1000 which results in a total winding resistance of 19.9Ω.

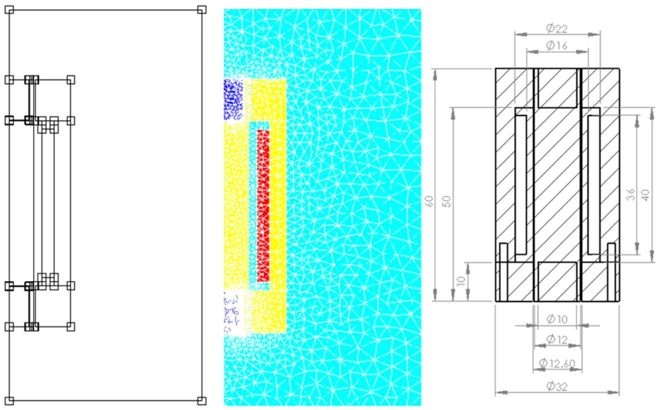

Fig. 6 The construction of the study domain by creating the necessary points and comparison with the structural drawings.

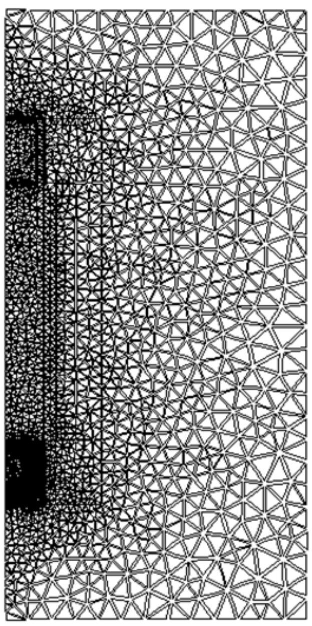

Fig. 7 The meshing in finite elements.

After sufficient FLUX2D simulations by trial-and-error approach, the most suitable dimensions for the proposed linear motor are determined and shown in Fig. 8. The corresponding lines of force of the magnetic field can be obtained as shown in Fig. 9. In addition, the magnetic flux density near the winding in units of Tesla can also be derived as shown in Fig. 10. From its numerical table, the average flux density can be determined. Consequently, the static force/stroke relation for a given excitation current can be numerically derived. Similar simulations may be repeated for different input currents and at different strokes of the plunger. Figure 11 shows the numerical static force/stroke relation for eight different excitation currents. In addition, the maximal output forces corresponding to different values of the input current for the developed linear motor are depicted in Table 1. Obviously, two design goals, which are 16 N output force and l mm linear working stroke, are successfully achieved. Finally, the photograph of the realized prototype is shown in Fig. 12.

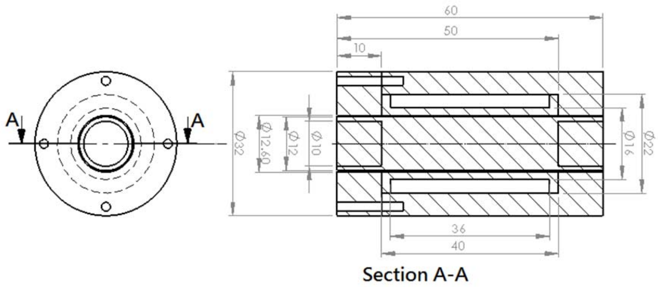

Fig. 8 The dimensions for the proposed novel linear motor.

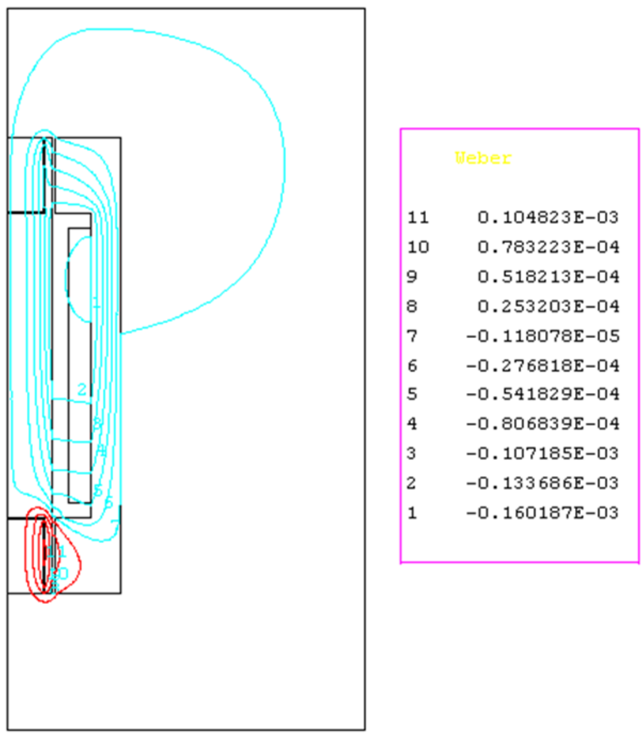

Fig. 9 The lines of force of the magnetic field (Input current: 0.25 A).

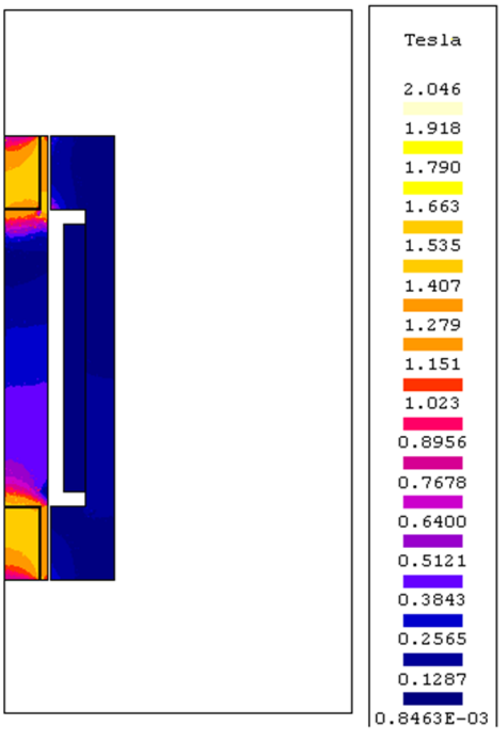

Fig. 10　The magnetic flux density in units of Tesla (Input current: 0.25 A).

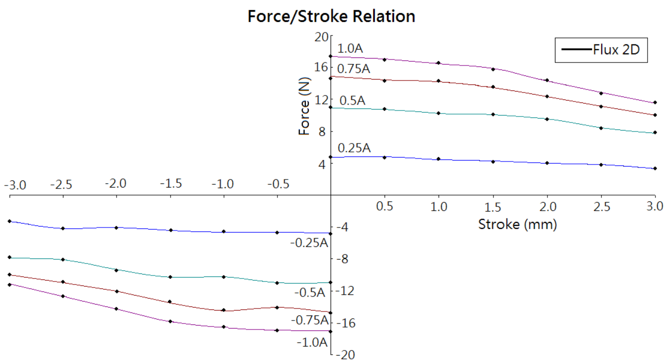

Fig. 11　The numerical static force/stroke relation for 8 different excitation currents.

Table 1　Simulation results of input current/ maximal output force for developed linear motor.

Input Current (A)	Max. Force (N)	Input Current (A)	Max. Force (N)
0.25	4.24	-0.25	-4.3
0.5	9.17	-0.5	-9.12
0.75	13.99	-0.75	-13.93
1	17.24	-1	-17.19

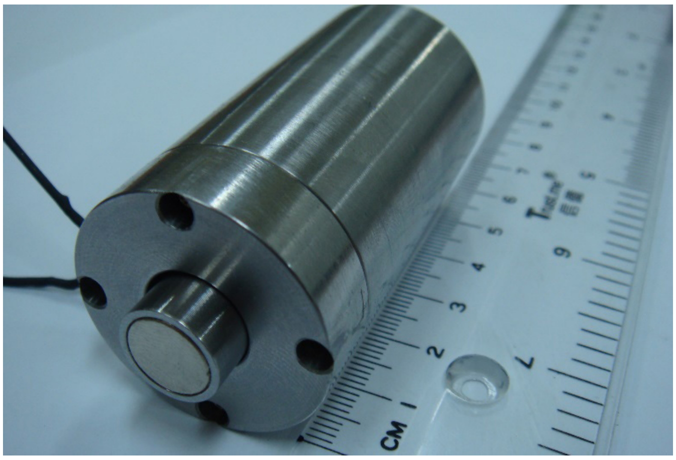

Fig. 12　Photograph of the realized prototype of linear motor.

3. EXPERIMENTAL TEST DEVICES

In this study, two experimental test devices are developed for evaluating the performance of the proposed linear motor. The first one is the static test rig as shown in Fig. 13. An open-loop controlled micro-stepping motor is utilized to control the position of plunger of the tested linear motor. The rotational angle and speed of the micro-stepping motor are derived directly from the number of pulses and the frequency of the generated pulse signal sent to the driver, respectively. In addition, the direction of rotation can be easily controlled by sending a Hi- (5 Volt) or Lo- (0 Volt) signal to one input port of the driver. Besides, the test device provides a position sensor (LVDT) as well as a load cell for the measurement of the stroke and the output force of the plunger. Finally, the control of the unit as well as the acquisition and processing of measured data are all integrated in a PC-based LabView software controller. The second one is the dynamic test device as depicted in Fig. 14. The output plunger of the tested linear motor drives a mass-spring-damper system, which is used to simulate the movement of the spool in a fluid power proportional valve body. The displacement of the mass is measured by a digital optical linear scale. Similarly, the control of this device as well as the data acquisition is all integrated in a PC-based LabVIEW software controller.

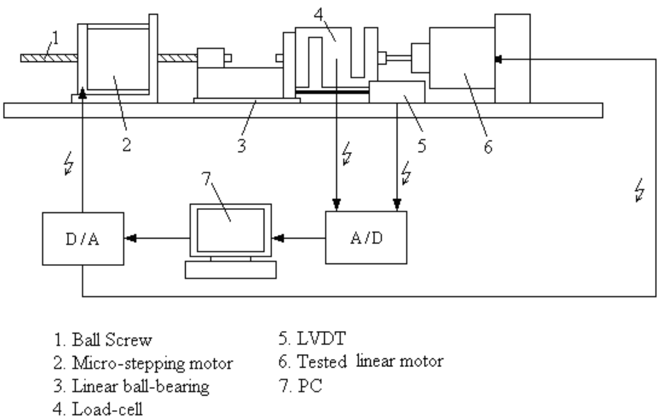

Fig. 13　The static force/stroke test device.

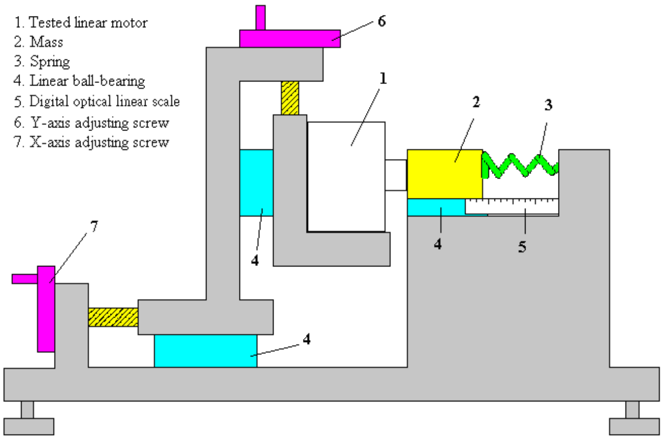

Fig. 14 The dynamic test device.

4. EXPERIMENTAL RESULTS AND DISCUSSION

The static output-force versus input-current relation of the proposed linear motor can be evaluated by using the static test device depicted in Fig. 14. The corresponding experimental results are shown in Fig. 15. Obviously, from Fig. 15, the output force of the developed linear motor is approximately proportional to the magnitude of the applied current. For example, the output force reaches 10 N for an input current of 0.5 A. On the other hand, the force/stroke family curves of the developed linear motor can also be measured by utilizing the same test device. Figure 16 shows the experimental results. For the maximal input current of 1.0 A, the maximal output force and the linear working stroke of the proposed linear motor are 16 N and 1.0 mm, respectively. It is also obvious that the output force approximately remains a constant within the linear working stroke, which is exactly the basic requirement for the design of a fluid power proportional valve. However, due to the compact design with smaller dimensions and lighter weight, the maximal output force of the proposed linear motor is somewhat smaller than that of a typical and commercially available proportional solenoid of a similar rating. Some quantitative comparisons are shown in Fig. 16 (Renn & Chen, 2005; Renn, Chen & Lu, 2008).

Other specifications associated with the proposed linear motor include hysteresis and dynamic time response. Figure 17 shows one typical experimental result for the evaluation of hysteresis, in which the force hysteresis is found to be around 3.2% for an input current of 1.0A. On the other hand, a typical experimental step response can also be obtained by using the dynamic test device and the result is shown in Fig. 18. The rise time for the waveform to go from 10% to 90% of its final position value is calculated to be 4.0 ms. The input current is set to be 1.0A. The externally connected mass is 107 g and the spring constant is 8.5 N/mm. The comparisons of the above-mentioned hysteresis and dynamic performance are also included in Fig. 19. Obviously, the overall performance of the proposed linear motor is superior to the target proportional solenoid made by Magnet-Schultz (Renn & Chen, 2005; Renn, Chen & Lu, 2008). Finally, the comparisons between simulation and experimental force/stroke results are shown in Fig. 20. It is noticeable that the simulation results agree quite well with the experimental ones. The maximal error is around 5 %. This proves the effectiveness of utilizing the software FLUX2D as the initial design tool.

5. CONCLUSION

In this paper, a novel linear motor is successfully developed and realized. After experimental tests, three conclusions may be drawn from this research.

1.For an input current of 1.0 A, the maximal output force and the linear working stroke of the linear motor are 16 N and 1.0 mm respectively, which are sufficient for the design of a fluid power proportional valve.

2.The dynamic test result shows that the rise time is 4 ms, which is obviously faster than that of a conventional proportional solenoid. Therefore, it is expected that such a new linear motor may find some potential application fields in fluid power proportional valve technology in the future.

3.The maximal error between simulation and experimental force/stroke results is around 5 %. This validates the accuracy of FLUX 2D simulations and proves that the FLUX 2D can be used as an effective tool to design electro-mechanical devices.

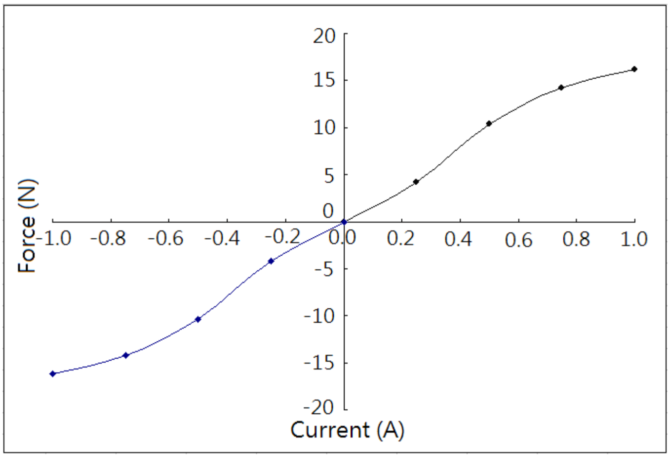

Fig. 15 The relation between output force and input current.

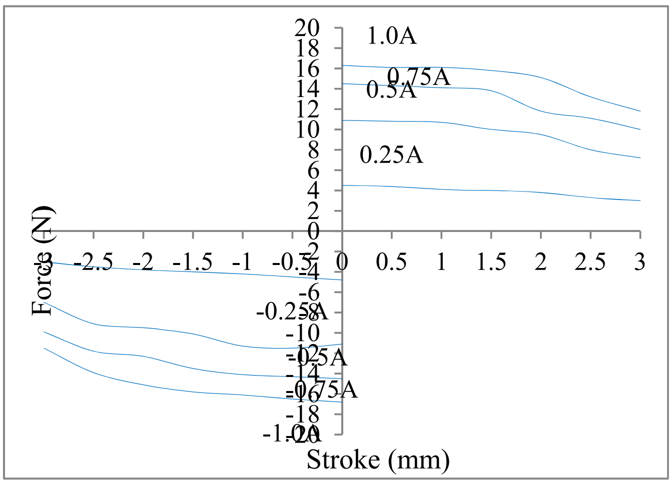

Fig. 16 Experimental force/stroke family curves of the developed linear motor

	Proposed novel linear motor	Proportional solenoid (G RFY 025 F20 B01)
Max. output force	16 N (1 A)	22 N (0.53 A)
Linear working stroke	1.0 mm	1.0 mm
Rise time (10% to 90% final value)	4 ms	14 ms
Hysteresis rated force	3.2 %	4.5 %
Output force type	Bi-directional	One-directional

Fig. 17 Quantitative comparisons between the proposed linear motor and the target proportional solenoid.

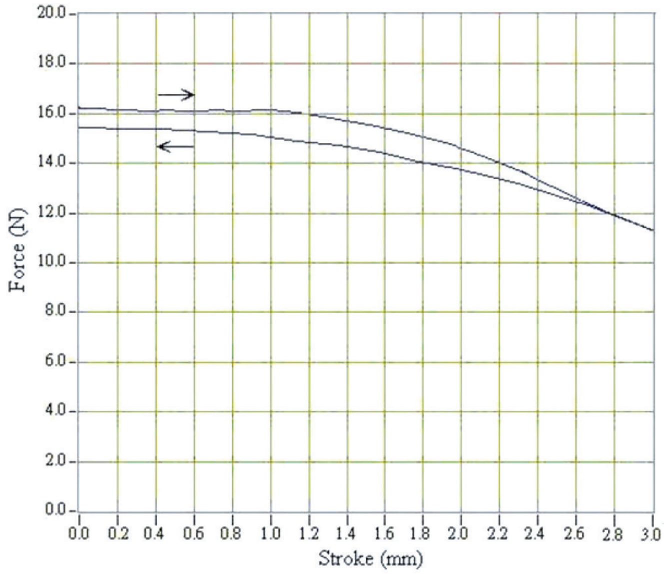

Fig. 18 Evaluation of output force hysteresis (Input current: 1.0A).

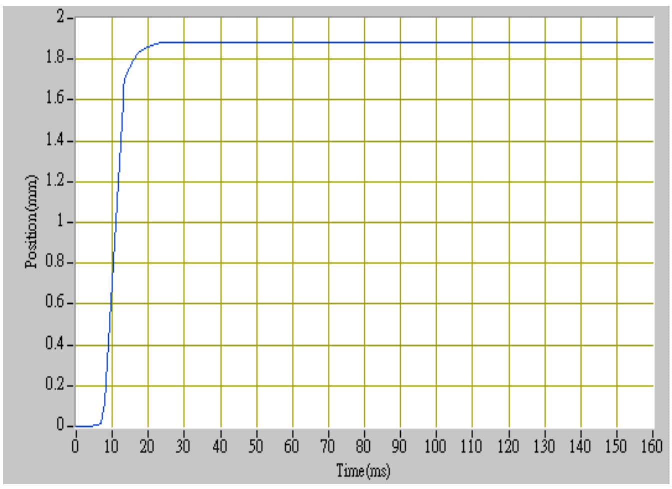

Fig. 19 Typical step response of the proposed linear motor (Input current: 1.0A).

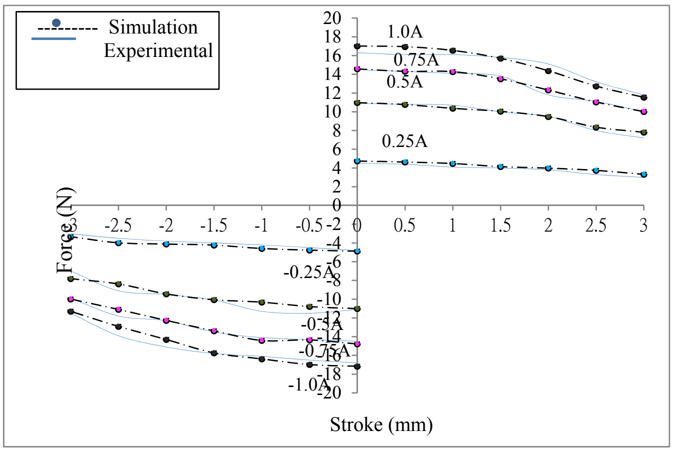

Fig. 20 Comparisons of simulation and experimental force/stroke results.

ACKNOWLEDGMENT

The authors gratefully acknowledge TEKTRO TECHNOLOGY Co., LTD, Taiwan, for providing all casting samples for testing.

REFERENCES

Backe, W. (1993). "Steuerungs-und Schaltungstechnik II."*Umdruck zur Vorlesung, RWTH Aachen, Germany (in German).*

Gamble, J., & Tappe, P. (2008). "A Novel bi-directional proportional hydraulic valve actuator." In *Proceedings Of The National Conference On Fluid Power* **51**, 301.

Li, Q., Ding, F., & Wang, C. (2005). "Novel bidirectional linear actuator for electrohydraulic valves." *IEEE transactions on magnetics,* **41**(6), 2199-2201.

Melin, J., & Quake, S. R. (2007). "Microfluidic large-scale integration: the evolution of design rules for biological automation." *Annual review of biophysics and biomolecular structure,* **36**(1), 213-231.

Mohith, S., Karanth, P. N., & Kulkarni, S. M. (2019). "Recent trends in mechanical micropumps and their applications: A review." *Mechatronics,* **60**, 34-55.

Renn, J. C., & Chen, H. M. (2005)." Design of a novel semi-active suspension for motorcycles with Fuzzy-sliding mode controller." *J. of the CSME,* **26**(3), 287-296.

Renn, J. C., Chen, C. Y., & Lu, C. H. (2008). "Gap control for a proportional floating vacuum pad. "*Proceedings of the Institution of Mechanical Engineers, Part C: Journal of Mechanical Engineering Science,* **222**(11), 2069-2076.

Renn, J. C., & Tsai, C. (2002). "Linearization of Force/Stroke Characteristic of Switching Solenoid Using Fuzzy-Logic-Controller." In *Proceedings of The Jfps International Symposium On Fluid Power*. The Japan Fluid Power System Society, **2002**(5-1), 193-198

Renn, J. C., & Xu, Z. L. (2003). "State-Space Modeling and FEM Design of a Moving-Coil Transducer for Fluid-Technical Proportional Valves. "*JOURNAL-CHINESE SOCIETY OF MECHANI-*

CAL ENGINEERS, **24**(2), 119-126.

Sugioka, H. (2010). "High-speed rotary microvalves in water using hydrodynamic force due to induced-charge electrophoresis." *Physical Review E,* **81**(3), 036301.

Yamahata, C., Lacharme, F., Burri, Y., & Gijs, M. A. (2005). "A ball valve micropump in glass fabricated by powder blasting." *Sensors and Actuators B: Chemical,* **110**(1), 1-7.

Zimmermann, K., Zeidis, I., & Lysenko, V. (2021). "Mathematical model of a linear motor controlled by a periodic magnetic field considering dry and viscous friction." *Applied Mathematical Modelling,* **89**, 1155-1162.